N and S Dual-Doped Mesoporous Carbon Nanostructure as a High Performance and Durable Metal Free Oxygen Reduction Reaction Electrocatalyst

Apichat Saejio[1], *Nattawan* Pitipuech[1], *Kultida* Kongpunyo[2], *Nutsuda* Buntao[2], *Kittimaporn* Nernprom[2], *Khemika* Boonkor[2], *Kitisak* Wichienwat[2], *Noppavan* Chanunpanich[3,4], *Narong* Chanlek[5], *Sangaraju* Shanmugam[6] and *Kriangsak* Ketpang[2,3*]

[1]Faculty of Engineering and Technology, King Mongkut's University of Technology North Bangkok Rayong Campus, Thailand
[2]Faculty of Science, Energy and Environment, King Mongkut's University of Technology North Bangkok Rayong Campus, Thailand
[3]Integrated Chemistry Research Center for Sustainable Technology (ICRT), Science and Technology Research Institute, King Mongkut's University of Technology North Bangkok, Thailand
[4]Department of Industrial Chemistry, Faculty of Applied Science, King Mongkut's University of Technology North Bangkok, Thailand
[5]Synchrotron Light Research Institute (Public Organization), Nakhon Ratchasima, Thailand
[6]Department of Energy Science & Engineering, Daegu Gyeongbuk Institute of Science & Technology (DGIST), Republic of Korea

Abstract. Discovering a high performance, durable, and cost-effective oxygen reduction reaction (ORR) electrocatalyst is a key strategy for widespread use of the high efficiency and environmentally friendly fuel cell and metal-air battery technologies. Herein, we fabricate a high performance and durable metal free N and S dual-doped mesoporous carbon nanostructure (NS-VXC) ORR catalyst using solid state thermolysis at 700 °C for 1 h. The fabricated catalyst exhibits nanocarbon aggregated chain-like morphology with a high surface area and mesoporous structure. The amount of N and S dopants embedded in mesoporous carbon nanostructure is found to be 3.2 and 1.1%, respectively which significantly attribute to the synergistic effect of spin and charge density leading to not only superior ORR performance but excellent durability in the alkaline environment as well. Rotating ring disk electrode analysis reveals the codoped NS-VXC catalyst possesses a direct 4-electron transfer number pathway with extremely low peroxide intermediate content. Compared to the benchmark Pt/C catalyst, the fabricated NS-VXC catalyst generated 10 mV ORR performance outperform and negligible performance degradation after the 10,000 ORR cycling test. These results suggest that an innovative solid state thermolysis methodology can be a powerful nanomaterial fabrication technique to generate high performance and excellent durability electrocatalyst for green energy applications.

Keyword. N and S codoped carbon, Metal free ORR catalyst, Oxygen reduction reaction, Fuel cell

1 Introduction

The electrochemical oxygen reduction reaction (ORR) is the key reaction directly determining the efficiency of the environmental compatibility energy conversion and storage technologies such as fuel cells and metal-air batteries [1]. Because of its sluggish kinetic, a substantial amount of catalyst is essentially required to kinetically dissociate the bonding of an oxygen molecule in the ORR process [1]. Currently, the precious platinum and/or platinum alloy nanoparticles supported on carbon (Pt/C) have been the most efficient and widely used as the major catalyst for reducing the overpotential of the ORR in both acids and alkaline media [2-4]. However, the nanoparticle Pt/C catalysts have several technical drawbacks such as high cost, CO poisoning, methanol crossover, and poor durability which significantly impede the current commercialization of fuel cell and metal-air technologies [5-6]. Thus, numerous innovative approaches have been intensively focused on the discovery of the high performance, excellent durability, and low-cost non-precious ORR electrocatalyst to replace the precious Pt/C catalyst [7-8].

Recently, carbon composite nanomaterials especially heteroatom doped carbon nanostructures have potentially shown as promising non-precious metal free ORRcatalyst due to their low cost, tunable surface chemistry, and facile electron transfer mobility [8]. Among heteroatoms dopants, nitrogen (N), similar in size to carbon, is the most widely investigated as the efficient dopant to promote the ORR [8]. It has been proposed that incorporation of a nitrogen atom into a carbon framework (NC) induces charge redistribution resulting in a slightly positive charge on carbon atoms adjacent to the doped nitrogen atom owing to the intrinsically higher electron negativity of nitrogen relative to carbon atoms [8]. The positively charged carbon atoms are capable of changing the chemisorption mode of an oxygen molecule from the

* Corresponding author: kriangsak.k@sciee.kmutnb.ac.th

usual end-on adsorption to side-on adsorption [8]. The diatomic oxygen adsorption can effectively weakening the O-O bond, facilitating oxygen reduction at the active nitrogen-doped carbon sites with lower ORR overpotential [8]. In this regard, various nanostructures of independent nitrogen-doped carbon (NC) catalysts have been studied as a possible replacement for Pt catalysts including N-graphene, N-CNTs, N-mesoporous carbon and N-nanoparticle carbon [8-9]. An excellent example of a nitrogen-doped carbon catalyst has been described by Gong et al. [9]. The nitrogen-doped vertically aligned carbon nanotubes (VA-NCNTs) electrocatalysts were prepared by pyrolysis of iron phthalocyanine under an NH_3 atmosphere and the obtained metal-free catalysts were subsequently investigated the ORR performance under alkaline media [9]. It was found that the metal-free VA-NCNTs promoted a direct 4-electron transfer ORR process with superior ORR activity relative to the precious Pt/C catalyst. In addition, the VA-NCNTs catalysts were much more stable to the CO poisoning and the methanol crossover in comparison with the precious Pt/C catalyst [9]. However, the number and specification of ORR active sites located in the prepared nitrogen-doped carbon electrocatalysts are preferentially altered when various kinds of carbon and nitrogen precursors are thermally carbonized at high temperatures, leading to unpredictable ORR performance.

Density functional theory (DFT) computation demonstrates that the overpotential of the ORR process dramatically decreases by additional co-incorporating sulfur (S) atom into the structure of NC electrocatalyst [10-11]. S atom possesses a similar electronegativity value as the C atom. Functionalizing a single S atom into a carbon structure contributes to the active positive charge on the doped S element owing to the mismatch of the outermost orbital of the S and C atoms [11]. Interestingly, simultaneous doping of S and N atoms into carbon nanostructure results in not only enhancing the active positive charge density but also substantially improving the spin density of the hexagonal C atom next to a doped N atom [11]. The synergistic effect of both asymmetrical spin and charge density contributes to substantially increasing the number of active C atoms, yielding superior ORR performance [11]. Experimentally, S and N atoms have been dually doped into carbon nanosheet [10, 12-13], carbon nanotube [14-15], three-dimensional carbon foam [16], two-dimensional graphitic sheet [17] by using high temperature pyrolyzing various kinds of carbon, nitrogen and sulfur resources under inert and/or the toxic ammonia gases. However, the ORR performance of the reported S and N codoped nanocarbon catalyst is still less competitive with the benchmark Pt/C catalyst [10-16].

Herein, we have developed a simple, cost-effective, and scalable method for fabricating a high performance and durable N and S codoped mesoporous carbon nanostructure (NS-VXC). The fabrication of the NS-VXC product was accomplished by solid state thermolysis a complex containing commercial carbon nanoparticle (VXC 72R), potassium thiocyanate (KSCN) and 2,2-bipyridine (BPD) at relatively low temperature under ambient atmosphere without applying any gas. The morphology and porous structure of the obtained products were systematically characterized by using a scanning electron microscope (SEM) and Brunauer–Emmett–Teller (BET) method, respectively. The amount of nitrogen and sulfur functional groups decorated in carbon structure was verified by the X-ray photoelectron spectroscope (XPS) technique. Then, the product was employed as a non-precious metal free catalyst to electrochemically promote the ORR in alkaline media using rotating ring disk electrode (RRDE) measurement. A novelty of this report is the synthesis method of the dual-doped N and S into porous carbon nanoparticles under solid state thermolysis conditions without purging any gases which have not been reported to date. In addition, the reported nanomaterial synthesis method is environmentally friendly, highly reproducible, template-free and easy to handle. It was found that the fabricated dual doped NS-VXC catalyst exhibited more highly active and durable to facilitate the ORR process than that of the precious Pt/C catalyst under alkaline media.

2 Experiments

2.1 Preparation of NS-VXC precursor

The NS-VXC precursor was prepared by modification of the synthesis method reported in the literature [18]. The carbon nanoparticles (VXC 72R) with an amount of 50 mg were added into a 50 ml flat bottom flask containing 25 ml ethanol. The admixture was ultrasonically dispersed for 30 min. At the same time, iron thiocyanate solution was prepared by dissolving 0.166 g $FeCl_3 \cdot 6H_2O$ and 0.29 g KSCN in 25 ml DI water. Once the carbon mixture was homogeneously dispersed, the iron thiocyanate solution was slowly transferred into the carbon slurry and the admixture was continually ultrasonicated for 60 min. After that, the bipyridine solution was prepared by dissolving 0.315 g 2,2-bipyridine in 10 ml ethanol and the obtained solution was poured into the carbon flask. The slurry flask was stirred for 20 h at room temperature. The solid product was collected by centrifuging the slurry at 13,000 rpm and finally drying at 80 ^oC overnight.

2.2 Synthesis of NS-VXC electrocatalyst

The dried NS-VXC precursor was finely ground using agate mortar and pestle. The fine powder was then transferred into a Hylok union cell and it was tightly sealed with another plug. A sample cell was put on a rectangular ceramic boat and it was delivered in the muffle furnace at the centre position. The heat treatment process was carried out at 700 ^oC for 1 h by maintaining the ramp rate at 10 $^oC\ min^{-1}$ under ambient conditions without purging any inert or ammonia gases. Once the calcination process was over, the sample was naturally cooled down to room temperature. The calcined sample was taken into a vial containing 1.0 M H_2SO_4 solution. The acid treatment process was programmed at 80 ^oC for 8 h to eliminate the unreacted species. The acid treated sample was collected by centrifuging the solution at 13,000 rpm and it was repeatedly washed with a large amount of DI water until the pH of the solution become neutral. The washed sample was then dried at 80 ^oC in

oven overnight and the dried sample was denoted as NS-VXC.

2.3 Physical characterizations

A field-emission scanning electron microscope (FE-SEM) was conducted using the Hitachi S-4800II instrument. SEM images were taken under an accelerated voltage condition of 3 kV, the sample must be coated with osmium before SEM investigation. Brunauer Emmett and Teller (BET) technique was participated to determine the surface area and pore diameter size of the catalysts. In BET analysis, the sample was purified by degassing at 150 °C for 8 h. Powder X-ray diffraction (XRD, PANalytical-Empyrean) technique with Kα radiation and generation voltage of 40 kV was acquired to verify the crystal structure of the samples. Moreover, the elemental compositions of catalysts were analyzed using X-ray photoelectron spectroscopy (XPS, Thermo Fisher Scientific, ESCALAB250 XPS system, Theta Probe XPS system) with monochromated Al Kα source at 15 kV and 150 W. Binding energy values on the X-axis were calibrated using C1s from a carbon value taken as 284.6 eV).

2.4 Electrochemical ORR characterizations

The electrochemical ORR performance of catalysts was estimated using a rotating ring disk electrode (RRDE) technique (Pine instrument). A three-electrode system comprised of glassy carbon, Pt wire and Ag/AgCl which functioned as working, counter and reference electrodes, respectively, were employed. The reference Ag/AgCl potential was converted to the reversible hydrogen electrode (RHE) potential following the equation reported in the literature [19]. The catalyst ink with the composition of 5 mg catalyst, 250 µL of DI-water, 20 µL of Nafion (5%), and 500 µL of isopropyl alcohol was ultrasonically dispersed for 30 min to obtain a homogenous ink [20-22]. The homogeneous ink was then carefully coated onto a clean RRDE electrode and left it dry under room temperature. The content of NS-VXC catalyst loaded on the working electrode was maintained at 0.4 mg cm^{-2}. For comparison, the noble Pt/C catalyst (10% Johnson Matthey) was taken to prepare catalyst ink and it was coated on an RRDE working electrode with an amount of 30 µg cm^{-2}. The ORR catalytic activity was conducted under an O_2-saturated 0.1 M KOH solution at a scan rate of 10 mV s^{-1}. RRDE experiments were repeatedly investigated at less than 3 times.

3 Results and Discussion

3.1 Fabrication of NS-VXC electrocatalyst

The porous N and S codoped carbon product was fabricated through a single-step doping method. The NS-VXC complex was easily prepared by solution mixing the commercial carbon nanoparticle, KSCN and 2,2-bipyridine compounds as carbon, sulfur and nitrogen resources, respectively. The collected fine precursor powder was subjected to solid state thermolysis at 700 °C for 1 h under autogenic pressure conditions without flowing gas. The impurity contained in the as-prepared sample was chemically treated using 1.0 M H_2SO_4 and the purified product was centrifugally separated and finally dried in an oven overnight. X-ray diffraction analysis was utilized to evaluate the crystal structure of the acid treated NS-VXC sample and the XRD pattern result is presented in Figure 1a. There were two peaks located at 2θ of 24.3 and 43.8 degrees, corresponding to the typical single phase of graphitic C(002) and C(100) planes of the turbostratic carbon structure. The fact that the C(002) plane of the carbon is generally center at 26.57 degree [23]. The C(002) plane for the prepared NS-VXC sample appeared at 2θ lower than that of the standard C(002) plane of the turbostratic carbon, indicating an increase in the interlayer spacing due to an increase in the d-spacing which is associated with the incorporation of N and S atoms into the graphitic layers of the carbon framework [23].

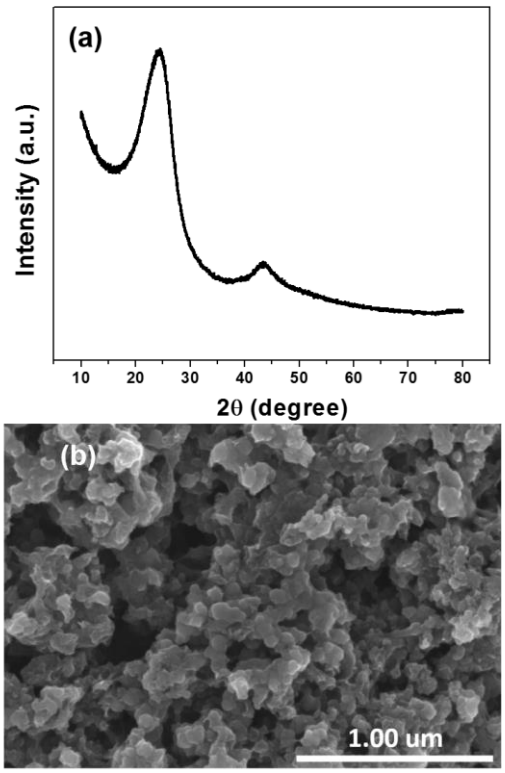

Figure 1 (a). X-ray diffraction pattern and (b) FE-SEM image of the acid treated NS-VXC sample

The morphology of the synthesized NS-VXC sample was subsequently determined using the FE-SEM technique and the SEM image of the acid treated NS-VXC sample is shown in Figure 1b. SEM image clearly reveals uniform nanosized particle connected chain-like structure which is a unique characteristic morphology of VXC 72R. The particle size was approximately in the range of 30-50 nm [21, 23]. In addition, the prepared NS-VXC sample exhibited noticeably high porosity which has benefit in the facile diffusion of reactant and product through the sample. It could be highlighted that thermal annealing of the NS-VXC precursor at 700 °C under autogenic pressure conditions resulted in the decomposition of sulfur and nitrogen precursors into individual atoms, whereas carbon is very stable, and it does not decompose under these

conditions. Atomized sulfur and nitrogen under solid state thermolysis conditions had high enough kinetic energy to randomly incorporate into carbon structure, maintaining the same morphology as the carbon host. This phenomenon was also observed in the morphology of doping heteroatom into graphene [12-13] and CNT materials [14-15].

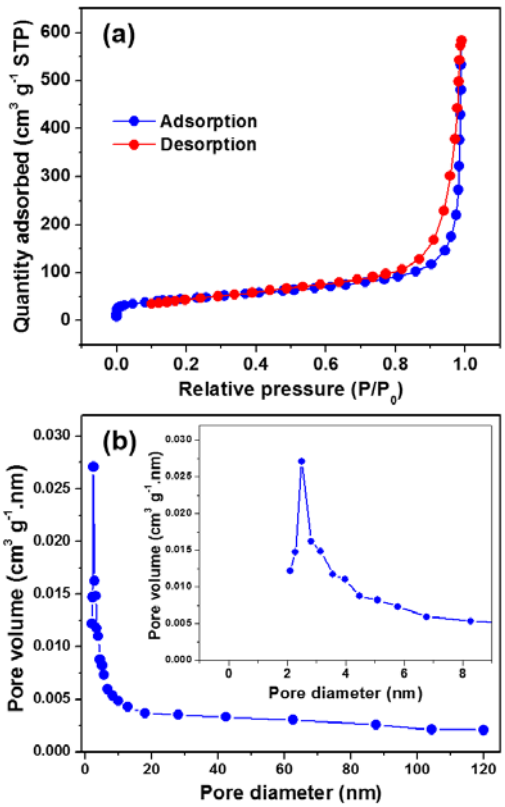

Figure 2 (a) Nitrogen adsorption/desorption isotherm and (b) the corresponding pore diameter size distribution of the acid treated NS-VXC sample

The porous structure and surface property of the acid treated NS-VXC sample was evaluated using the BET technique and the sorption isotherm and pore diameter size distribution results are depicted in Figure 2. The nitrogen sorption isotherm result of the purified NS-VXC sample displays the obvious hysteresis loop, suggesting that the sorption isotherm of the NS-VXC sample was of type IV [24]. According to the International Union of Pure and Applied Chemistry (IUPAC) classification, the formation of the hysteresis loop indicates the capillary condensation taking place in the mesopores [24]. Furthermore, the maximum pore volume of the synthesized NS-VXC sample was found at a pore diameter size of 3 nm (inset Figure 2b). Basically, pore diameter size smaller than 2 nm is classified as micropores, between 2 to 50 nm are known as mesopores and larger than 50 nm are called macropores [24]. Nitrogen adsorption/desorption isotherm and pore size distribution results suggested the calcined NS-VXC product was a mesoporous structure. The BET surface area of the prepared NS-VXC samples was calculated to be 232 m^2 g^{-1}. It has been reported that a catalyst with a mesoporous structure is capable of effectively facilitating the diffusion of the reactant in the ORR process [11, 13].

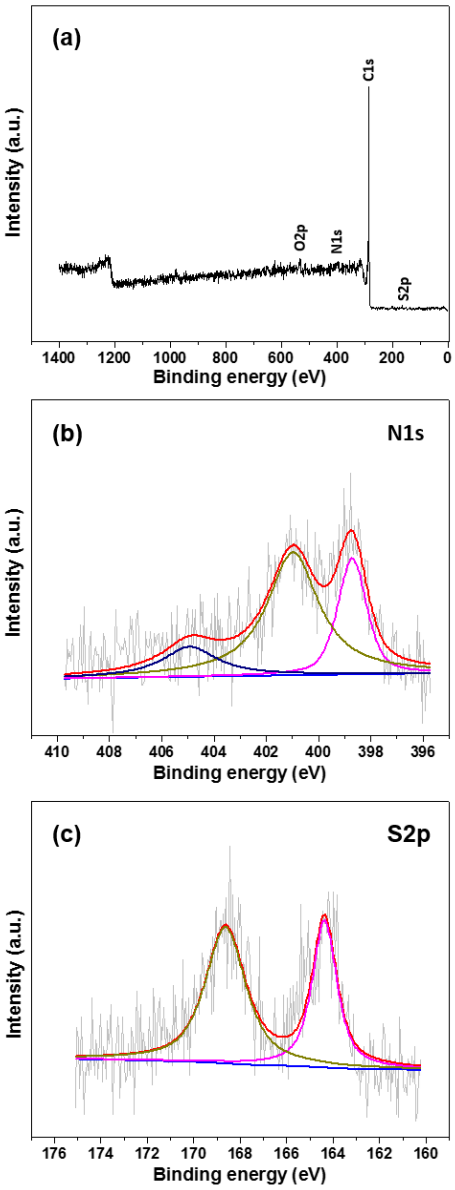

Figure 3 (a) XPS survey spectra, (b) deconvoluted XPS N1s spectra and (c) S2p XPS spectra of NS-VXC sample.

To verify the elemental compositions decorated in the prepared NS-VXC sample, the XPS experiment was acquired and XPS results are displayed in Figure 3. In XPS survey spectra (Figure 3a), elements C, N, S, and O were apparently observed. The presence of N and S elements in the purified NS-VXC sample indicate that N and S atoms were successfully doped into the carbon structure of the synthesized NS-VXC sample. The content of C, N, S and O elements presented in the NS-VXC sample was 93.7, 3.2, 1.1 and 2.0%, respectively. The fact that ferric ion was also added in the preparation of NS-VXC precursor. However, there was no information on Fe species in the XPS survey spectra (Figure 3a), indicating Fe species was not incorporated into carbon structure during the solid state thermolysis process and the

remaining Fe compound was totally removed during the acid treatment process. Figure 3b shows the deconvoluted N1s XPS spectra of the prepared NS-VXC sample. The deconvoluted N1s XPS result provided 3 peaks at a binding energy of 398.7, 400.9 and 404.3 eV, which were corresponding to pyridinic-type, pyrrolic-type and graphitic-type nitrogen, respectively [23]. Figure 3c represents the deconvoluted S2p XPS spectra of the purified NS-VXC sample. The deconvoluted S2p XPS spectra generated 2 peaks at a binding energy of 164.3 and 168.4 eV [14]. The peak at a binding energy of 164.3 eV was indexed to a thiophene-like structure where a sulfur atom is embedded between two carbon atoms (C-S-C) [14]. On the other hand, the peak at a binding energy of 168.4 eV was associated with an oxidized sulfur (C-SO_X-$C_)$ species that has been proven to be ORR inactive [11]. It has been mentioned that the incorporation of a higher electronegativity N atom into a lower electronegativity carbon atom is attributed to relatively high positive charge density on the adjacent sp^2-bond carbon atoms. Especially, pyridinic-type nitrogen wherein nitrogen atoms present at the edge of the carbon framework bind to two carbon atoms majorly responsible for an ORR active site [11]. On the other hand, the S atom has an identical electronegativity value as the C atom. Doping a single S atom into the C framework resulted in the actively positive charge on the S atom mainly due to the mismatch of the outermost orbital of the S and C atoms [11]. Furthermore, simultaneous incorporation of both electron accepting N atom and S atom into carbon structure significantly contributed to the synergistic effects of asymmetrical spin and charge density which substantially increase the number of active C atoms, yielding superior ORR performance [11].

3.2 Electrochemical ORR performance of NS-VXC catalyst

Next, the purified NS-VXC sample was employed as electrocatalyst material to promote the ORR process in an alkaline solution. The homogeneous NS-VXC catalyst ink was firstly prepared by dispersing the calcined NS-VXC powder in the mixture solution of DI water, isopropyl alcohol and Nafion. A drop of the catalyst slurry was uniformly coated on a clean RRDE working electrode. The amount of NS-VXC catalyst on the RRDE working electrode was kept constant at 0.4 mg cm^{-2}. The catalyst coated RRDE working electrode was then assembled into an electrochemical cell equipped with a Pt wire as counter electrode and an Ag/AgCl as reference electrode under O_2 saturated 0.1 M KOH solution. Figure 4 presents ORR polarization plots using the linear swept voltammogram technique (LSV) for the dual-doped NS-VXC catalyst (Figure 4a) in comparison with LSV results obtained from the undoped commercial carbon nanoparticle (VXC) (Figure 4b) and the benchmark Pt/C (Figure 4c) catalysts at a rotation speed of 800 to 2,000 rpm and 10 mV s^{-1} scan rate under O_2 saturated 0.1 M KOH solution. It was found that the current density for the codoped NS-VXC (Figure 4a), pristine VXC (Figure 4b) and Pt/C (Figure 4c) catalysts noticeably enhanced when the rotation speed was raised from 800 to 2,000 rpm. This typical observation is principally attributed to the shortening flux-diffusion distance at high rotating speeds [23].

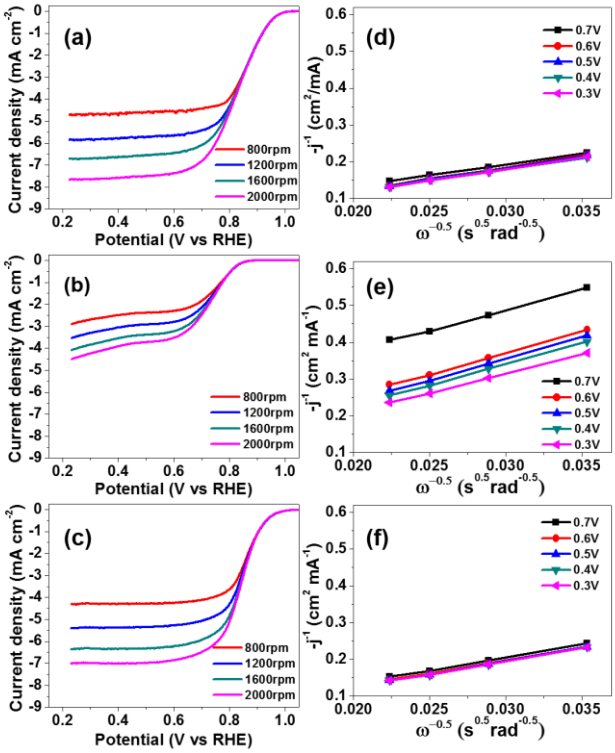

Figure 4 ORR polarization plots conducted by linear sweep voltammograms (LSV) for (a) NS-VXC, (b) VXC and (c) Pt/C catalysts in 0.1 M KOH at 10 mV s^{-1} at various electrode rotation speeds. Corresponding Koutecky-Levich (K-L) plots at different electrode potentials of (d) NS-VXC, (e) VXC and (f) Pt/C catalysts

To verify the ORR kinetic for the catalysts, inversion of current density (j^{-1}) and rotation speed ($\omega^{-0.5}$) at different electrode potentials was qualitatively plotted known as Koutecky-Levich (K-L) plot. The K-L plot results for the codoped NS-VXC (Figure 4d), undoped VXC (Figure 4e) and the commercial Pt/C (Figure 4f) catalysts over the potential range of 0.3 to 0.7 V were linear and parallel, implying the number of electron transfer facilitating ORR process in that potential range was same [23]. Particularly, the K-L plot results obtained from the dual doped NS-VXC (Figure 4d) and the benchmark Pt/C catalysts were almost identical over the potential range of 0.3 to 0.7 V, suggesting the ORR kinetic catalyzed by the dual-doped NS-VXC catalyst was definitely as efficient as promoted by the expensive Pt/C catalyst. The number of electron transfer values calculated from the slope of K-L plots for NS-VXC, VXC and Pt/C catalysts at a potential of 0.5 V was found to be 4.0, 3.1 and 4.0 respectively, suggesting that the fabricated NS-VXC catalyst promotes the ORR process with a directed-four electron transfer number which is as sufficient as the noble Pt/C catalyst.

In order to compare the ORR electrocatalytic activity as well as to understand the mechanism insight about the ORR process, LSV measurement using the RRDE technique was carried out for the codoped NS-VXC catalyst as compared to undoped VXC and the noble Pt/C catalysts at a rotation speed of 1,600 rpm in O_2-saturated 0.1 M KOH solution and the corresponding ring and disk

current density is presented in Figure 5a. The content of the inexpensive NS-VXC and VXC catalysts loaded on the RRDE working electrode was about 0.4 mg cm^{-2} while the amount of expensive Pt/C catalyst coated on the working electrode was 30 μg cm^{-2}. The performance of the ORR electrocatalyst can be monitored by 3 major parameters: onset potential (E_{on}), half-wave potential ($E_{1/2}$) and liming current density (I_L) and these parameters can be directly extracted from the disk current density. The ORR onset potential (E_{on}) determines the capability of the catalyst to promote the ORR process. The larger number of E_{on} values indicates a highly efficient electrocatalytic material to accelerate the ORR process. The smaller number of the E_{on} value implies the inefficient ORR catalyst. The E_{on} value observed for the dual-doped NS-VXC, undoped VXC and the noble Pt/C catalysts was found to be 1.01, 0.88 and 1.02 V vs RHE, respectively. In comparison, the E_{on} value extracted from the dual-doped NS-VXC catalyst was 130 mV larger than that of the undoped VXC catalyst and eventually the fabricated NS-VXC catalyst exhibited comparable E_{on} value to that of the benchmark Pt/C catalyst. This means that the fabricated codoped NS-VXC catalyst was greatly effective to facilitate the ORR process similar to the noble Pt/C catalyst. In addition to the E_{on} value, half-wave potential ($E_{1/2}$) is a key potential directly determining the ORR reaction rate. The larger number of $E_{1/2}$ values is responsible for the faster ORR kinetic. The less value of $E_{1/2}$ suggests the sluggish ORR kinetic. In this study, the $E_{1/2}$ value was measured at a disk current density of -3 mA cm^{-2}. the $E_{1/2}$ value obtained for the codoped NS-VXC, undoped VXC and the benchmark Pt/C catalysts was about 0.86, 0.63 and 0.85 V vs RHE, respectively. The codoped NS-VXC catalyst exhibited 230 mV greater the $E_{1/2}$ value than that of the undoped VXC catalyst. Compared to the expensive Pt/C catalyst, the ORR performance of the inexpensive NS-VXC catalyst was 10 mV outperform. Obviously, simultaneous incorporation of both N and S atoms into carbon nanostructure resulted in substantially improving the ORR kinetic rate and eventually overcoming the ORR performance of the benchmark Pt/C catalyst. Besides, E_{on} and $E_{1/2}$, limiting current density (I_L), implies the diffusion rate of the reactant O_2 molecule and ORR product (OH^- compound) through the surface of the catalyst material. The greater I_L value indicates a more highly efficient catalyst to electrochemically reduce reactant O_2 molecule into the OH^- product in the ORR process. In other words, the small number of I_L means unpreferable catalyst material to promote the ORR process. The number of I_L values at potential 0.3 V vs RHE for the codoped NS-VXC, undoped VXC and the noble Pt/C catalysts was found to be -7.2, -3.8 and -6.3 mA cm^{-2}, respectively. The synthesized dual-doped NS-VXC catalyst generated the highest I_L value relative to undoped VXC and the expensive Pt/C catalysts, suggesting a more favourable ORR electrocatalyst in alkaline media.

The outstanding E_{on}, $E_{1/2}$ and I_L values for the prepared codoped NS-VXC catalyst significantly derived from the simultaneous incorporation of N and S atoms into the C structure. Embedding a single N atom into a carbon framework creates an active positive charge on the neighbouring sp^2-bond carbon atoms [11]. In particular, pyridinic-type N has been accepted as the main major ORR active site [11, 23]. On the other hand, the presence of the S atom in the carbon structure leads to an active positive charge on the S atom due to the mismatch of the outermost orbital of the S and C atom [11]. Interestingly, simultaneous codoping of N and S atoms into the carbon framework significantly resulted in the synergistic effects of asymmetrical spin and charge density which substantially improved ORR performance [11]. Not only an electronic effect, but the mesoporous structure and the high surface area of the prepared dual-doped NS-VXC catalyst were essentially responsible for the superior ORR as well.

Generally, the mechanism for the ORR process under alkaline media can be either direct pathway or indirect pathway processes. In direct pathway mechanism, oxygen molecule gains 4-electron transfer directly and electrochemically reduces to OH^- species as the product. In the indirect pathway route, the ORR process is divided into 2 steps. In the first step, the oxygen molecule receives two electron transfers, generating peroxide (HO_2^-) species as an intermediate compound. In the second step, the intermediate HO_2^- compound electrochemically receives another 2-electron transfer to complete the ORR process. Therefore, the amount of peroxide intermediate and the number of electrons transfers can be used to classify the ORR mechanism route. The direct pathway mechanism route requires a 4-electron transfer number with less content of peroxide species. However, a high amount of intermediate compound with low content of electron transfer number suggests an indirect pathway mechanism process. The content of the peroxide intermediate and electron transfer numbers can be calculated based on the ring and disk current density obtained from RRDE measurement at a rotation speed of 1,600 rpm in an O_2-saturated 0.1 M KOH solution. As shown in Figure 5a, the ring current density value of the dual doped NS-VXC and Pt/C catalysts was similar, while, the pristine VXC catalyst generated a much higher ring current density value than those of the codoped NS-VXC and Pt/C catalysts. This implied that the fabricated dual doped NS-VXC catalyst accelerated the ORR process with less amount of peroxide compound. The actual content of OH_2^- species and the number of electron transfers are displayed in Figure 5b. It was found that the amount of intermediate OH_2^- species (blue color) of the dual-doped NS-VXC catalyst was about 2% which is similar to the content of peroxide species derived from the precious Pt/C catalyst. On the other hand, the undoped VXC catalyst delivered a peroxide content of about 40%. The calculated electron transfer number (red color) for the dual doped NS-VXC, pristine VXC and precious Pt/C catalyst were 4.0, 3.2 and 4.0 respectively. The number of electron transfers obtained from RRDE measurement was consistent with the electron transfer number derived from the K-L plot. It is clearly mentioned that the non-precious N and S codoped carbon catalyst was able to electrochemically reduce oxygen via a direct 4-electron reduction pathway in an alkaline medium.

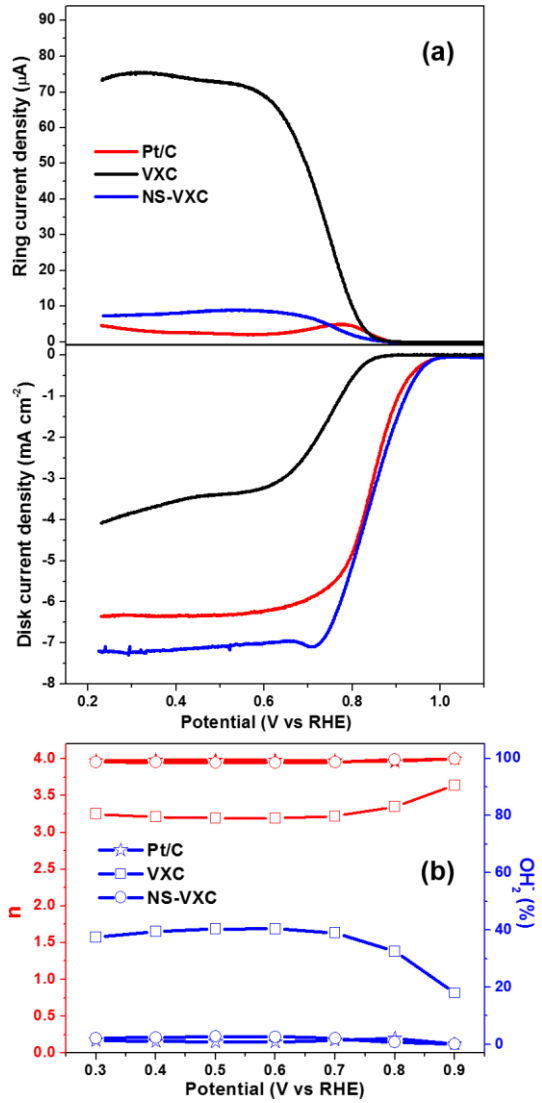

Figure 5 (a) LSVs measurement of NS-VXC, VXC and Pt/C (10% Pt/C, Johnson Matthew) catalysts obtained from rotating ring disk electrode measurement in O_2-saturated 0.1 M KOH at a sweep rate of 10 mV s^{-1}, 1,600 rpm and (b) Percentage of peroxide and the electron transfer number of catalyst at various electrode potential.

The durability is an important parameter indicating the performance degradation of the catalyst during ORR operation. Figure 6 compares the ORR performance degradation of the non-precious NS-VXC catalyst after 10,000 cyclic durability studies at a potential range of 0.6-1.0 V vs RHE with a scan rate of 50 mV s^{-1} in alkaline solution. It was found that the degradation of the number of $E_{1/2}$ values for the codoped NS-VXC catalyst was 1 mV (at a current density of -3 mA cm^{-2}) after 10,000 cycles of durability evaluation. The fabricated NS-VXC catalyst exhibited much durability to perform ORR in alkaline solution. It has been reported that the ORR performance of the noble Pt/C catalyst drastic decayed by 50 mV after 5,000 cycles of durability determination [23]. Pt nanoparticles supported on carbon easily aggregate each other becoming large particles [4]. The large particle size directly results in the obvious reduction of catalyst surface area, yielding less ORR active size and eventually low ORR activity [4]. Moreover, Pt dissolution and carbon oxidation during the accelerated durability test were also noticeably attributed to the degradation of the ORR performance of the noble Pt/C catalyst [5].

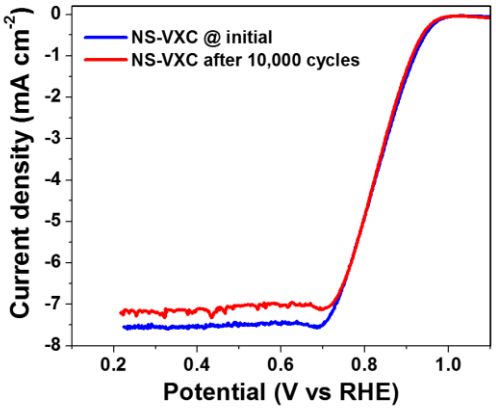

Figure 6 Polarization curves of fabricated NS-VXC catalyst during cycling durability test in O_2-saturated at 1,600 rpm (cycling test were carried out in potential range 0.6 - 1.0V vs RHE with 50 mV s^{-1} in 0.1 M KOH)

4 Conclusion

We succeeded in fabricating N and S codoped into porous carbon nanostructure as a high performance and durable metal free ORR catalyst using a simple and scalable method. The metal free catalyst was obtained by pyrolysis of the nitrogen, sulfur and carbon derived complex at 700 °C for 1 h under autogenic pressure conditions. The acid treated product exhibited a relatively high surface area with mesoporous structure as well as a large number of N and S dopants embedded into the carbon framework. The fabricated catalyst was subsequently electrochemically investigated the ORR performance using the RRDE technique in alkaline media. The N and S codoped carbon (NS-VXC) catalyst exhibited much more efficiency to facilitate the ORR process than the undoped carbon (VXC) and eventually the ORR performance of the dual doped NS-VXC catalyst was outperform the benchmark Pt/C catalyst. Furthermore, the fabricated NS-VXC catalyst demonstrated a highly durable ORR cycling test for 10,000 cycles with negligible performance loss.

Acknowledgements

This research was funded by King Mongkut's University of Technology North Bangkok, Contract no. KMUTNB-65-NEW-06.

References

[1] A. Kulkarni, S. Siahrostami, A. Patel, J. K. Nørskov, Understanding catalytic activity trends in the oxygen reduction reaction, Chemical Reviews, 118(5) (2018):2302-2312.
[2] M. Shao, Q. Chang, J.P. Dodelet, R. Chenitz, Recent advances in electrocatalysts for oxygen reduction reaction, Chemical reviews, 116(6) (2016):3594-3657.

[3] Y.J. Wang, N. Zhao, B. Fang, H. Li, X.T. Bi, H. Wang, Carbon-Supported Pt-Based Alloy Electrocatalysts for the Oxygen Reduction Reaction in Polymer Electrolyte Membrane Fuel Cells: Particle Size, Shape, and Composition Manipulation and Their Impact to Activity, Chemical reviews, 115(9) (2015):3433-3467.
[4] H. Yano, M. Kataoka, H. Yamashita, H. Uchida, M. Watanabe, Oxygen reduction activity of carbon-supported Pt-M (M = V, Ni, Cr, Co and Fe) alloys prepared by nanocapsule method, Langmuir, 23(11) (2007):6438-6445.
[5] H. Yano, M. Watanabe, A. Iiyama, H. Uchida, Particle-size effect of Pt cathode catalyst on durability in fuel cells, Nano Energy, 29 (2016):323-333.
[6] S. Cherevko, N. Kulyk, K. J.J. Mayrhofer, Durability of platinum-based fuel cell electrocatalysts: Dissolution of bulk and nanoscale platinum, Nano energy, 29 (2016) : 275-298.
[7] A.A. Gewirth, J.A. Varnell, A.M. DiAscro, Nonprecious metal catalyst for oxygen reduction in heterogeneous aqueous systems, Chemical reviews, 118(5) (2018):2313-2339.
[8] L. Dai, Y. Xue, L. Qu, H.J. Choi, J.B. Baek, Metal-free catalyst for oxygen reduction reaction, Chemical reviews, 115(11) (2015):4823-4892.
[9] K. Gong, F. Du, Z. Xia, M. Durstock, L. Dai, Nitrogen-doped carbon nanotube arrays with high electrocatalytic activity for oxygen reduction, science, 323(5915) (2009):760–764.
[10] Y. Guo, S. Yao, L. Gao, A. Chen, M. Jiao, H. Cui, Z. Zhou, Boosting bifunctional electrocatalyst activity in S and N co-doped carbon naosheets for high-efficientcy Zn-air batteries, Journal of Materials Chemistry A, 8(8) (2020):4836-4395.
[11] J. Liang, Y. Jiao, M. Jaroniec, S. Z. Qiao, Sulfur and nitrogen dual-doped mesoporous graphene electrocatalyst for oxygen reduction with synergistically enhanced performance, Angewandte Chemie International Edition, 51(46) (2012):11496-11500.
[12] J. Li, Y. Zhang, X. Zhang, J. Huang, J. Han, Z. Zhang, X. Han, P. Xu, B. Song, S, N dual-doped graphene-like carbon nanosheet as efficient oxygen reduction reaction electrocatalyst, ACS Applied Materials & Interfaces, 9(1) (2017):398-405.
[13] K. Qu, Y. Zheng, S. Dai, S. Z. Qiao, Graphene oxide-polydopamine derived N, S-codoped carbon nanosheets as superior bifunctional electrocatalyst for oxygen reduction and evolution, Nano Energy,19 (2016):373-381.
[14] Q. Shi, F. Peng, S. Liao, H. Wang, H. Yu, Z. Liu, B. Zhang, D. Su, Sulfur and nitrogen co-doped carbon nanotubes for enhancing electrochemical oxygen reduction activity in acidic and alkaline media, Journal of Materials Chemistry A, 1(47) (2013):14853-14857.
[15] C. Dominguez, F.J P. Alonzo, S.A.A. Thabaiti, S.N. Basahel, A.Y. Obaid, A.O. Alyoubi, J.L.G. Fuente, S. Rojas, Effect of N and S co-doping of tytymultiwalled carbon nanotubes for the oxygen reduction, Electrochimica Acta, 157 (2015):158-165.
[16] Z. Liu, H. Nie, Z. Yang, J. Zhang, Z. Jin, Y. Lu, Z. Xiao, S. Huang, Sulfur-nitrogen co-doped three-dimensional carbon foams with hierarchical pore structures as efficient metal-free electrocatalysts for oxygen reduction reactions, Nanoscale, 5(8) (2013):3283-3288.
[17] C. Hu, L. Dai, Multifunctional carbon-based metal-free electrocatalyst for simultaneous oxygen reduction, oxygen evolution, and hydrogen evolution, Advanced Materials, 29(9) (2017):160492-16050.
[18] P. Chen, T. Zhou, L. Xing, K. Xu, Y. Tong, H. Xie, L. Zhang, W. Yan, W. Chu, C. Wu, Y. Xie, Atomically dispersed iron-nitrogen species as electrocatalysts for bifunctional oxygen evolution and reduction reactions, Angew Angewandte Chemie, 129(2) (2017):610-614.
[19] T. S. J. Wang, C. Qiu, X. Ling, B. Tian, W. Chen, C. Su, B, N codoped and defect-rich nanocarbon material as a metal-free bifunctional electrocatalyst for oxygen reduction and evolution reactions, Advanced Science, 5(7) (2018):1800036-1800045.
[20] J. Sanetuntikul, K. Ketpang, S. Shanmugam, Hierarchical nanostructured Pt_8Ti-TiO_2/C as an efficient and durable anode catalyst for direct methanol fuel cells, ACS Catalysis, 5(12) (2015):7321-7327.
[21] K. Ketpang, A. Boonkitkoson, N. Pitipuech, C. Poompipatpong, J. Sanetuntikul, S. Shanmugam, Highly active and durable transition metal-coordinated nitrogen doped carbon electrocatalyst for oxygen reduction reaction in neutral media, E3S Web of Conferences, 14 (2019):01005.
[22] K. Ketpang, J. Prathum, P. Juprasat, W. Junla, K. Wichianwat, A. Saejio, C. Poompipatpong, N. Chanunpanich, Electrochemical oxygen reduction reaction performance of water hyacinth derived porous non-precious electrocatalyst in alkaline media, E3S Web of Conferences, 14 (2019):01004.
[23] J. Sanetuntikul, S. Shanmugam, High pressure pyrolyzed non-precious metal oxygen reduction catalyst for alkaline polymer electrolyte membrane fuel cells, Nanoscale, 7(17) (2015):7644-7650.
[24] K. S. W. Sing, Reporting physisorption data for gas/solid systems with special reference to the determination of surface area and porosity, Pure and applied chemistry, 54(11) (1982):2201-2218.

* Corresponding author: kriangsak.k@sciee.kmutnb.ac.th